Electrodeposition and Corrosion Resistance of Ni-W-B Coatings

C.P. Steffani, J.W. Dini, J.R. Groza, and A. Palazoglu

A ternary nickel-base alloy Ni-W-B has been developed for surface corrosion and wear resistance to replace chromium plating, which uses environmentally hazardous solutions. The deposition conditions used an alkaline bath and insoluble anodes. The as-deposited alloy typically contains 40 wt% W and 1 wt% B and has an amorphous or partially amorphous structure. These deposits compare favorably with hexavalent chromium deposits in throwing power, color uniformity, and reflectivity. The corrosion resistance of Ni-W-B alloy was compared with hexavalent chromium and electroless nickel deposits in a variety of acids, including hydrochloric, sulfuric, fluoroboric, and phosphoric. In all cases, best results were obtained with the Ni-W-B deposits.

1. Introduction

Chromium plating has been used extensively as a surface finish for applications that demand wear and corrosion resistance. Although chromium coatings are hard, aesthetically pleasing, and durable, the plating solutions are toxic and present a risk to human health and the environment.

Electrodeposited nickel-base ternary alloys have been developed and used as viable chromium substitutes (Ref 1, 2). Specifically, electrodeposited Ni-W-B alloys have surface finish and wear properties similar to those of chromium platings. As-plated coatings have a hardness of approximately 600 HV, but annealing increases their hardness. Phase changes and mechanical property evolution in Ni-W-B alloys were addressed in a previous paper (Ref 1). The maximum hardness of about 900 HV, which is comparable to the hardness of chromium, occurred during postplating heat treatment at 400 °C. The initial metastable structure decomposed into fine particles of Ni_4W in a nickel solid solution, while the amorphous matrix crystallized. Heating to higher temperatures coarsened grain size and led to decreasing hardness.

The coatings that develop maximum hardness values are particularly suitable for wear-resistant applications. When Ni-W-B deposits are used for other purposes, such as surface corrosion or decorative purposes, the meaningful properties of alternative deposits are surface quality and corrosion resistance.

The main focus of the present work is to identify the role of electrodeposition processing conditions of Ni-W-B alloys to achieve good engineering characteristics of the deposits, such as good surface finish and corrosion resistance, particularly when exposed to acids. For this purpose, characterization of the plating process and of the microstructure and properties of deposits has been performed.

C.P. Steffani and **J.W. Dini,** Manufacturing and Materials Engineering Division, Lawrence Livermore National Laboratory, Livermore, CA 94550, USA; **J.R. Groza** and **A. Palazoglu,** Department of Chemical Engineering and Materials Science, University of California, Davis, CA 95616, USA.

2. Experimental

2.1 Process Description

The plating solution, prepared from concentrated AMPLATE UA-B (Fidelity Chemical Company, Newark, NJ), consisted of sodium tungstate, nickel sulfate, and sodium borate. Brightening and wetting agents were used. The use of brighteners was aimed at achieving thinner deposits with maximum reflectivity. Sodium laurel sulfate was used to reduce the surface tension at the cathode and allow easy release of hydrogen bubbles. The pH was adjusted with ammonium hydroxide to 8.4. Ammonia also chelates the metal ions and stabilizes the bath. Chemicals were replenished periodically.

The plating rate was adjusted by varying the current density. Steel panels, masked on one side with platers' tape, acted as the cathodes. For reflectivity and coating uniformity studies, cathodes were made of polished copper. The anodes were insoluble 300-series stainless steel. They can either be placed in membrane baskets to prevent electrolyte oxidation or used directly in the solution. When used directly, without a membrane barrier, the anodes required periodic carbon treatment to remove the brightener breakdown by-products. The process operating temperature was 50 °C. The solution was agitated and filtered to ensure alloy uniformity and reduce deposit roughness due to suspended particulate matter. Cathode current density varied from 0.039 to 0.108 A/cm^2, depending on the shape and the rate of deposition required.

2.2 Process Characterization

Throwing power was measured by the ability of the bath to completely plate the inside corner of a bent plate. Copper panels, 5 by 40 cm with a 90° bend 20 cm from one end, were used for this purpose.

2.3 Deposit Characterization

Color uniformity was determined by plating a polished copper panel and comparing color versus thickness. Deposit reflectivity was assessed by measuring the intensity of reflected light impinged on the surface at an angle of incidence 5° from the perpendicular. The light comprised wavelengths corresponding to natural sunlight.

Corrosion resistance tests were carried out in five types of acids: 25% HCl, 25% H_2SO_4, 25% HNO_3, 48% HBF_4, and 5% H_3PO_4. The measured corrosion times were extrapolated to 25.4 μm/year thickness loss.

Atomic absorption spectroscopy (AAS) was used for bulk alloy elemental analysis. Deposit microstructure was determined using x-ray diffraction (XRD) and transmission electron microscopy (TEM) associated with selected-area diffraction (SAD). The XRD studies used a Scintag diffractometer (Scintag, Inc., Cupertino, CA 95014) with Cu-Kα radiation. For TEM work, 3 mm disks were mechanically thinned, followed by ion milling. The TEM/SAD studies employed a Philips 400 microscope (Phillips Electronic Instruments, Mahwa, NJ) operated at 120 kV.
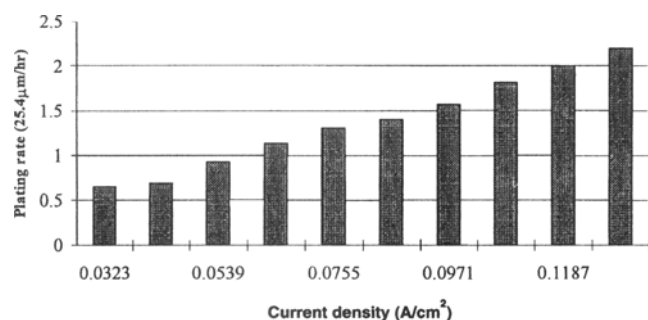

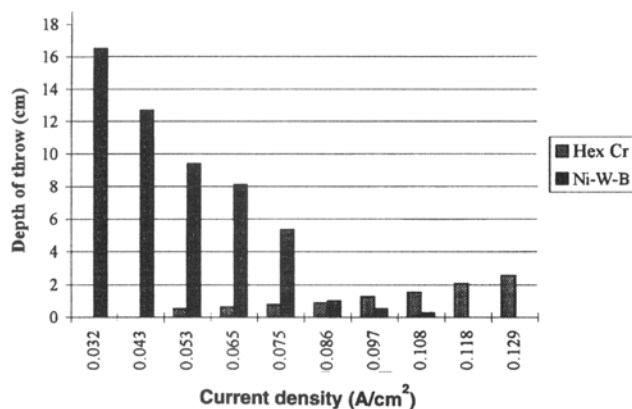**Fig. 1** Plating rate variation with current density

Fig. 2 Throwing power as a function of current density for Ni-W-B and hexavalent chromium baths
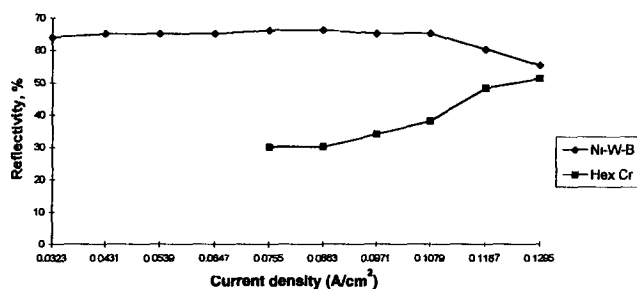

Fig. 3 Reflectivity of Ni-W-B and chromium deposits as a function of current density

3. Results

The cathode efficiency in the electrodeposition processing was about 38% and was dependent on the current density and electrolyte replenishment through the double layer at the cathode. The variation of the plating rate as a function of current density is shown in Fig. 1. For the range used, current density variation does not affect the alloy composition and structure. Plating rate dictates the final thickness of the electroplated foils. The thickness can be varied between 1 and 250 μm, depending on deposition time. The throwing power variation with current density is shown in Fig. 2. For comparison, the throwing power of a hexavalent chromium bath is also shown.

Chemical analysis by AAS indicated 39.5 wt% W and 1 wt% B in the plated coating. Reflectivity results of Ni-W-B alloys showed little variation (between 55 and 66%) with the current density values used (Fig. 3). These results were compared with those of hexavalent chromium deposits. In this case, no plating was obtained below 0.075 A/cm^2. Above this current density, reflectivity increased directly with current density.

Color uniformity of Ni-W-B platings was bright for all current densities used up to 0.108 A/cm^2 (Table 1). At 0.108 A/cm^2, the deposit was partially bright, becoming frost-burnt at a current density of 0.129 A/cm^2. As a comparison, the hexavalent chromium deposit became bright only at a current density of 0.118 A/cm^2.

The corrosion resistance of Ni-W-B coatings in various acids is shown in Table 2. For comparison, corrosion resistance test results also are provided for hexavalent chromium and phosphorous electroless nickel.

The XRD scan for a similar as-plated Ni-W-B alloy is shown in Fig. 4. One intense peak, centered at 44°, corresponds to the Ni (111) reflection. A crystal size calculated from the Scherrer formula based on the (111) peak breadth is about 3 to

Table 1 Color uniformity of Ni-W-B and chromium deposits

Current density, A/cm^2	Ni-W-B	Hexavalent chromium
0.0323	Bright	No plate
0.0431	Bright	No plate
0.0539	Bright	No plate
0.0647	Bright	No plate
0.0755	Bright	Dull
0.0863	Bright	Dull
0.0971	Bright	Frost
0.1079	Bright/frost	Frost
0.1187	Frost	Bright
0.1295	Frost/burnt	Bright

Table 2 Corrosion resistance in acids(a)

Acid	Ni-W-B	Hexavalent chromium	11% electroless nickel
25% HCl	0.25	100	1
25% H_2SO_4	0.25	25	0.75
25% HNO_3	0.65	0.1	80
48% HBF_4	0.1	0.2	1.5
5% H_3PO_4	0.3	4	0.8

(a) Corrosion times extrapolated to 25.4 μm/year thickness loss.

4 nm. Figure 5 shows the TEM micrograph and SAD pattern for an as-plated foil. The SAD pattern indicates diffuse, continuous rings, which are characteristic for a very fine-grained and possibly amorphous structure. Very fine grains may also be responsible for less sharp diffraction rings in SAD patterns of nanocrystalline materials.

4. Discussion

The electroplating conditions used in this work show that Ni-W-B coatings can be deposited from an alkaline bath using insoluble anodes. The cathode efficiency of Ni-W-B deposition was calculated to be three times better than for hexavalent chromium deposition. It is also higher than the electrode efficiency of other alloy (e.g., Ni-W-P) electroplating processes (18 to 25%) (Ref 3). This higher coulombic efficiency and the alkalinity of the plating solution generate no hazardous fumes and less corrosivity than hexavalent chromium processing solutions. Similarly, the throwing power of Ni-W-B compares very favorably with that of chromium deposition (Fig. 2), enabling better uniformity of the deposit thickness. Consequently, the alternative Ni-W-B coatings exhibited better finish properties than chromium. Both color uniformity and reflectivity of Ni-W-B deposits were substantially better than those of the chromium counterparts.

The chromium replacement alloys typically contain 40 wt% W and 1 wt% B (Ref 1, 2). The XRD peak broadening (Fig. 4) and diffuse rings of such alloys in TEM/SAD analysis (Fig. 5) indicate a very fine grain structure. Some nanometer-range crystals were observed in the TEM micrograph (Fig. 5). More detailed studies of a similar coating by high-resolution electron microscopy showed nanometer-size crystalline grains in an amorphous matrix of nickel-base solid solution (Ref 4). Boron is the main amorphizing addition (Ref 5). The final microstructure is a supersaturated solid solution in which all tungsten is dissolved in the nickel matrix. In equilibrium conditions, the solubility limit of tungsten into the nickel matrix is only 26%. This supersaturation may also contribute to the amorphous structure. The supersaturation in the electrodeposited alloy may be attributed to a high bath temperature (50 °C) during electrochemical processing. Such amorphous, structureless coatings may reproduce very precisely the characteristics of the surface on which they are deposited. Therefore, a bright surface was obtained when Ni-W-B was deposited on polished copper substrates.

The main benefit in using the Ni-W-B alternative coating is its strongly enhanced acid corrosion resistance. As shown in Table 2, the corrosion resistance of Ni-W-B alloy is one or two orders of magnitude better than that of chromium in HCl, H_2SO_4, and H_3PO_4. In Table 2, corrosion times are extrapolated to 25.4 µm/year thickness loss. The corrosion resistance of Ni-W-B alloys is also better than that of electroless Ni-11P alloy. This improved corrosion resistance may be first attributed to a greater throwing power and hence better uniformity of the deposited layer. Secondly, an amorphous structure usually offers better corrosion resistance than a crystalline counterpart. Yao et al. (Ref 3) measured a uniform oxide film about 4 nm deep when amorphous Ni-W-P coatings were corrosion tested in a salt solution. The homogeneous structure in

the amorphous phase without grain boundaries or phase separation certainly favors the formation of such a uniform passive oxide layer. A uniform tungsten distribution was detected in a similar Ni-W-B alloy in a previous study (Ref 1). The presence of both tungsten and boron may stabilize the coating against oxidation.

5. Conclusions

Alternative Ni-W-B alloys with 40 wt% W and 1 wt% B can be deposited from an alkaline bath using insoluble anodes. These deposits compare favorably with hexavalent chromium in throwing power, color uniformity, reflectivity, and acid corrosion resistance. These enhanced properties may be attributed to a nanocrystalline, perhaps partially amorphous structure that consists of a supersaturated solution of tungsten in the nickel matrix.
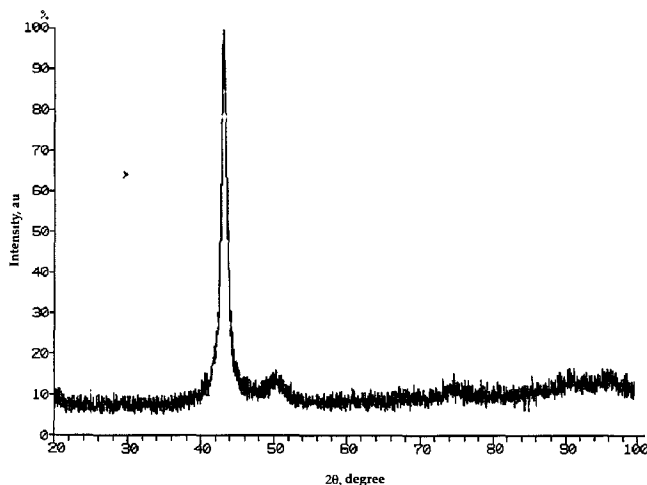
Acknowledgments

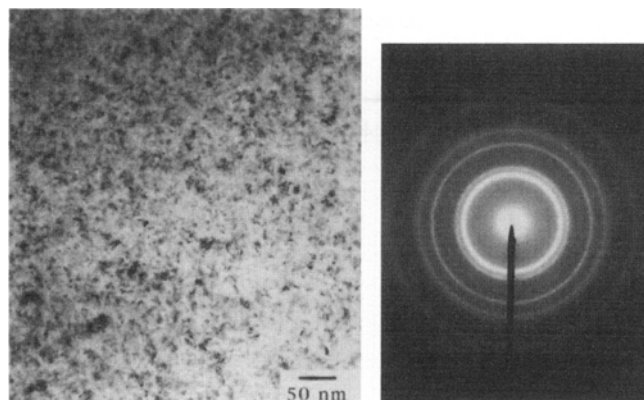**Fig. 4** XRD pattern of as-plated deposit

Fig. 5 TEM micrograph and SAD pattern for as-plated Ni-W-B alloy

References

1. G. Graef, K. Anderson, J.R. Groza, and A. Palazoglu, Phase Evolution in Electroplated Ni-W-B Alloy, *Mater. Sci. Eng. B*, in press

2. D. Scruggs, G. Croopnick, and J. Donaldson, brochure, Amorphous Technologies International, undated

3. S. Yao, W. Zhou, H. Guo, and M. Kowaka, Corrosion Behavior of Electrodeposited Amorphous Ni-W-P Films, *Corrosion, Electrochemistry, and Catalysis of Metastable Metals and Intermetallics*, Vol 93-30, C.R. Clayton and K. Hashimoto, Ed., Electrochemical Society, 1993, p 108-118

4. D. Scruggs, Amorphous Technologies International, personal communication, 1994

5. P.S. Kumar and P.K. Nair, X-Ray Diffraction Studies on the Relative Proportion and Decomposition of Amorphous Phase in Electroless Ni-B Deposits, *Nanostruct. Mater.,*, Vol 4, 1994, p 183